A Dynamic Bayesian and Machine Learning Framework for Quantitative Evaluation and Prediction of Operator Situation Awareness in Nuclear Power Plants

Shuai Chen[a], Huiqiao Jia[a], Tao Qing[a], Li Zhang[a] and Xingyu Xiao[b,c,*]

[a]Hunan Institute of Technology, Hunan, 421002, China
[b]Institute of Nuclear and New Energy Technology, Tsinghua University, Beijing, 100084, China
[c]National Key Laboratory of Human Factors Engineering, Beijing, 100094, China

ARTICLE INFO

Keywords:
Situation awareness (SA)
Dynamic Bayesian network (DBN)
Human reliability
Performance shaping factors (PSFs)
Nuclear power plant (NPP)

ABSTRACT

Operator situation awareness is a pivotal yet elusive determinant of human reliability in complex nuclear control environments. Existing assessment methods, such as SAGAT and SART, remain static, retrospective, and detached from the evolving cognitive dynamics that drive operational risk. To overcome these limitations, this study introduces the dynamic Bayesian–machine learning framework for situation awareness (DBML-SA), a unified approach that fuses probabilistic reasoning and data-driven intelligence to achieve quantitative, interpretable, and predictive situation awareness modeling. Leveraging 212 operational event reports (2007–2021), the framework reconstructs the causal–temporal structure of 11 performance shaping factors across multiple cognitive layers. The Bayesian component enables time-evolving inference of situation awareness reliability under uncertainty, while the neural component establishes a nonlinear predictive mapping from PSFs to SART scores, achieving a mean absolute percentage error of 13.8 % with statistical consistency to subjective evaluations ($p > 0.05$). Results highlight training quality and stress dynamics as primary drivers of situation awareness degradation. Overall, DBML-SA transcends traditional questionnaire-based assessments by enabling real-time cognitive monitoring, sensitivity analysis, and early-warning prediction, paving the way toward intelligent human–machine reliability management in next-generation digital main control rooms.

1. Introduction

Situation awareness (SA) represents an operator's perception, comprehension, and projection of system states in a given operational context, and it is widely recognized as a critical determinant of human reliability and safety performance in complex socio-technical systems. In nuclear power plants (NPPs), especially within digital main control rooms, operators are required to interpret a vast amount of information from advanced display systems, execute highly proceduralized tasks, and coordinate with automation systems under strict time constraints. The modernization of control room technologies, characterized by higher automation levels, denser information displays, and more integrated interfaces, has substantially increased the cognitive demands on human operators.

Traditional approaches to evaluating SA, such as the situation awareness global assessment technique (SAGAT) Endsley (1988) and the situation awareness rating technique (SART) Taylor (2017), have provided useful insights into the cognitive performance of operators. However, these methods are inherently static, subjective, and scenario-dependent, relying heavily on self-reports or post-trial questionnaires Xiao, Liang, Tong and Wang (2024). Consequently, they are incapable of representing the temporal evolution and causal dependencies that underlie operator cognition and decision-making processes during dynamic operational or accident scenarios Xiao, Zhu, Liang, Tong and Wang (2025c). To ensure reliable human performance in future digitalized NPPs, it is therefore necessary to develop quantitative, time-dependent, and interpretable models of operator SA.

Despite significant progress in cognitive modeling and human reliability analysis (HRA), several key challenges remain unresolved in SA assessment. First, current models rarely incorporate causal dependencies among multiple performance shaping factors (PSFs) Xiao, Qi, Liu, Chen, Liang, Tong and Wang (2025b), such as training quality,

*The research was supported by a grant from the scientific research foundation of Hunan provincial education department (24B0830), doctoral research foundation of Hunan institute of technology (HQ23009), and the science and technology innovation program of Hunan province (2023RC3195).

*Corresponding author
xxy23@mails.tsinghua.edu.cn; +86-10-62784836 (X. Xiao)
ORCID(s): 0009-0009-1926-3592 (X. Xiao)

teamwork, interface design, task complexity, and stress. These interdependencies play a decisive role in how operators perceive and interpret system information, yet they are often simplified or treated independently. Second, most existing approaches cannot capture the time-dependent evolution of SA during transient or accident conditions Boring, Joe and Mandelli (2015). Operator cognition and attention fluctuate dynamically as the task progresses, but traditional probabilistic safety models treat human performance as a static probability. Third, there is a lack of quantitative validation that bridges subjective evaluation (e.g., questionnaire-based SA scores) and objective physiological evidence (e.g., eye-tracking or electrodermal activity) Logothetis and Pauls (1995). This absence limits both the interpretability and credibility of current SA measurement approaches.

To address these challenges, this study aims to develop a hybrid data-driven framework that quantitatively evaluates and predicts operator situation awareness levels in NPP control rooms. The proposed dynamic Bayesian–machine learning framework (DBML-SA) integrates three complementary methodological components: (1) Statistical analysis of event data, to extract causal relationships among PSFs from historical human performance information; (2) dynamic Bayesian Network (DBN) modeling, to represent the probabilistic and temporal dependencies governing SA degradation or maintenance; and (3) Machine learning–based prediction of SART scores, to enable data-driven estimation of SA levels using measurable cognitive and contextual indicators. Together, these components enable both causal interpretation and predictive capability, bridging the gap between qualitative psychological constructs and quantitative reliability modeling.

This research makes three major contributions to the modeling and quantitative evaluation of operator SA in nuclear power plants:

- **Causal Modeling of SA Factors.** A data-driven causal model was constructed based on 212 operation event reports (2007–2021), systematically identifying 11 key PSFs and quantifying their interdependencies that influence operator SA.
- **Dynamic Bayesian and Physiological Integration.** A dynamic Bayesian network (DBN) was developed to incorporate both static PSFs and dynamic physiological indicators, enabling time-resolved inference of SA reliability and its temporal evolution.
- **Machine Learning–Based Prediction and Validation.** A neural network model was trained to predict SART-based SA scores from PSF inputs, and validated through simulator-based steam generator tube rupture (SGTR) experiments, showing consistent trends between predicted and measured SA levels.

The DBML-SA framework was validated through simulator-based SGTR experiments, demonstrating consistent trends between model-predicted and measured SA levels. By integrating probabilistic reasoning and data-driven learning, this study provides a robust and interpretable foundation for real-time SA monitoring and cognitive reliability evaluation in advanced digital control environments.

The remainder of this paper is organized as follows. Section 2 reviews traditional and emerging methods for evaluating operator SA. Section 3 introduces the proposed hybrid framework, detailing its overall architecture, data preprocessing, statistical modeling, DBN construction, experimental validation, and machine learning–based prediction module. Section 4 presents the results and analysis, including temporal inference of SA reliability, diagnostic reasoning, and sensitivity analysis, validation against subjective assessments, and predictive performance of the neural network model. Section 5 discusses the theoretical and practical implications of the framework for dynamic HRA and intelligent operator support in digital control rooms. Finally, Section 6 concludes the study and outlines potential directions for future research, including multimodal data integration, semantic knowledge representation, and real-time visualization of SA dynamics.

2. Literature Review

2.1. Traditional situation awareness evaluation methods

SA represents the operator's ability to perceive environmental elements, comprehend their meaning, and project future system states within a given time and space. The concept, first formalized by Endsley Endsley (2021), is structured as a three-level hierarchical model: (i) perception of the elements in the environment, (ii) comprehension of the current situation, and (iii) projection of future status based on that understanding. These levels describe a progressive cognitive process through which operators transform sensory input into contextual knowledge and

anticipatory reasoning, thereby supporting accurate decision-making under time-critical and information-intensive conditions Endsley, Garland et al. (2000).

In the context of HRA Xiao, Chen, Qi, Zhao, Liang, Tong and Wang (2025a), SA has been widely recognized as a determinant of human performance reliability. Failures of SA, whether at the perception, comprehension, or projection level, can propagate into operational errors and safety-critical events. Reason's Swiss-cheese model Larouzee and Le Coze (2020) conceptualizes such failures as latent conditions that erode defensive barriers, allowing unsafe acts to penetrate the system. From a cognitive-systems perspective, Wickens and Hollnagel Parasuraman, Sheridan and Wickens (2008) have emphasized that SA reflects the interaction between human information processing capacity and task demands within a dynamic environment Ramsey, Jansma, Jager, Van Raalten and Kahn (2004); Osman (2010). Consequently, degraded SA often manifests as delayed diagnosis, incorrect procedure selection, or ineffective team coordination Gorman, Cooke and Winner (2017), all of which are well-documented precursors to human error in nuclear, aviation, and process-control domains.

In nuclear power plant operations, maintaining adequate SA is particularly challenging due to the system's complexity, time-varying dynamics, and high consequences of failure Zhang and Horigome (2001). Operators must continuously monitor hundreds of interacting parameters, interpret alarms and procedural instructions, and coordinate actions under tight temporal constraints. The transition from analog to digital and now to intelligent control rooms has further altered the distribution of cognitive workload between humans and automation De Ambroggi and Trucco (2011). While advanced automation reduces manual burden, it can also introduce new challenges such as automation complacency, out-of-the-loop performance, and mode confusion, each of which has been linked to SA degradation Alberti, Agarwal, Gutowska, Palmer and de Oliveira (2023). Empirical studies in digital nuclear environments have shown that fluctuations in attention, stress, and interface complexity can significantly modulate the operator's momentary SA, in turn affecting task performance and error probability Li, Zhang, Dai and Li (2017).

Accordingly, modern HRA frameworks increasingly regard SA as a latent state variable that mediates the effect of performance-shaping factors (PSFs) on human error probability Kim, Park, Jung, Jang and Seong (2015). Quantifying this state and its dynamic evolution has thus become a central challenge for reliability analysis in digital control rooms. However, most existing approaches remain limited to static checklists or post-hoc surveys, lacking both temporal resolution and causal interpretability. A quantitative, data-driven model that captures the dynamic dependencies among PSFs, automation level, physiological state, and SA is therefore essential to advance human-centric safety assessment in next-generation nuclear power operations.

2.2. Probabilistic and Data-Driven Models in HRA

With the increasing complexity and automation of NPP operations, probabilistic and data-driven modeling approaches have gained prominence in HRA. These approaches aim to quantify the uncertainty and dynamics of human performance beyond traditional deterministic or expert-based methods.

Early generations of HRA methods, such as the technique for human error rate prediction (THERP) Kirwan (1983), standardized plant analysis risk–human reliability analysis (SPAR-H) Gertman, Blackman, Marble, Byers, Smith et al. (2005), and the more recent integrated decision-tree human event analysis system–error causal analysis (IDHEAS-ECA) Zhang, Yang, Yin and Liu, introduced structured frameworks for estimating human error probabilities (HEPs) within probabilistic risk assessments (PRAs). THERP established the foundation by using fault-tree–like decompositions to assign error probabilities based on expert judgment and limited empirical data. SPAR-H further incorporated PSFs Park, Jung and Kim (2020), including stress, time pressure, complexity, and experience, to adjust nominal error probabilities through multiplicative modifiers. IDHEAS-ECA, developed under the U.S. Nuclear Regulatory Commission, represented an evolution toward cognition-based modeling, explicitly linking observable PSFs to cognitive processes such as detection, diagnosis, and decision-making. Despite these advances, these models generally treat human actions as static events and rely heavily on expert-derived data, offering limited capability to reflect the time-dependent evolution of operator cognition or real-time adaptation to changing conditions Xiao et al. (2025a).

To overcome these constraints, recent studies have introduced BN and DBN Shiguihara, Lopes and Mauricio (2021) formulations into HRA. BNs enable representation of complex causal dependencies among PSFs, cognitive states, and observable behaviors through probabilistic graphical structures. This approach facilitates bidirectional inference, allowing both forward prediction of error likelihood and backward diagnosis of influential causes, while updating beliefs as new evidence becomes available. The dynamic extension DBN further captures temporal dependencies between successive cognitive states, providing a natural framework for modeling how attention, workload, or stress

fluctuate over time. Applications of BN/DBN approaches have been reported in domains such as control room teamwork assessment, situational diagnosis, and dynamic error propagation, demonstrating improved interpretability and adaptability compared with conventional static models.

In parallel, the rapid advancement of machine learning and artificial intelligence techniques Li, Liang, Wang, Luo, Chen, Liao, Wei, Deng, Xu, Zhang et al. (2024) has provided new avenues for operator state recognition and cognitive performance prediction. Neural networks, support vector machines (SVMs), random forests, and recurrent architectures such as long short-term memory (LSTM) Graves (2012) networks have been employed to infer operator workload Xiao, Qi, Liang, Tong, Deng and Chen (2023), fatigue, or decision accuracy from multimodal data including eye-tracking, physiological signals, and control interface logs Kasneci, Kübler, Broelemann and Kasneci (2017). These data-driven methods exhibit strong pattern recognition and nonlinear mapping capabilities, allowing them to capture high-dimensional correlations that are difficult to model analytically.

Nevertheless, purely data-driven models often lack explainability and causal interpretability, whereas traditional probabilistic frameworks provide transparency but limited adaptability Xiao et al. (2024). Bridging these two paradigms has therefore become a central research direction in modern HRA. In this context, the present study proposes a hybrid framework that integrates Bayesian causal reasoning with machine learning–based prediction, enabling both interpretable causal inference and data-driven estimation of operator situation awareness in dynamic nuclear control room environments.

2.3. Bayesian and Markov Frameworks for Dynamic Probabilistic Modeling

Probabilistic graphical models Koller and Friedman (2009) provide a powerful formalism for representing and reasoning about uncertainty in complex systems. Among them, Bayesian networks and Markov Chung (1967) models are two fundamental approaches that enable the encoding of causal dependencies and temporal dynamics in a mathematically consistent way. This section introduces the theoretical foundations of static Bayesian networks, Markov chains, and their integration into dynamic Bayesian networks (DBNs), which serve as the probabilistic backbone of the proposed framework Nagarajan, Scutari and Lèbre (2013).

2.3.1. Static Bayesian Network

A Bayesian Network (BN) integrates the principles of probability theory and graph theory, offering an effective approach for uncertainty reasoning. It captures deterministic, stochastic, and imprecise dependencies among a set of variables through a directed acyclic graph (DAG) composed of three key components: (i) nodes and directed arcs, (ii) prior probabilities, and (iii) conditional probabilities Deng, Xiao, Zhu, Cao, Liu, Zhang, Huang, Yu, Jiang and Liu (2023).

Each node represents a random variable, and each directed arc denotes a dependency relationship. If an arc points from node A to node B, A is called the parent node of B, and B is the child node of A. Nodes without parents are referred to as root nodes, characterized by their prior probabilities. The probability of event B occurring given the occurrence of event A is referred to as the conditional probability.

Probabilistic reasoning in a BN involves both qualitative and quantitative aspects. The qualitative structure is represented by nodes and directed arcs reflecting causal or correlational relationships among variables, while the quantitative part is defined through conditional probability tables (CPTs) that specify the probabilistic dependencies between a node and its parent nodes.

Assuming the network consists of random variables $X = \{X_1, X_2, \dots, X_n\}$, the joint probability distribution can be expressed as:

$$P(X_1, X_2, \dots, X_n) = \prod_{i=1}^{n} P(X_i | \mathrm{Pa}(X_i)) \tag{1}$$

where $\mathrm{Pa}(X_i)$ denotes the set of parent nodes of variable X_i.

2.3.2. Markov Model

A Markov model describes stochastic processes that evolve over time based on the Markov property, i.e., the future state depends only on the present state and not on the sequence of past states. A discrete-time Markov chain can be defined as a triplet (S, A, π), where:

- S represents the state space, consisting of all possible system states $\{s_1, s_2, \dots, s_N\}$.

- $A = [a_{ij}]$ denotes the state transition probability matrix Eddy (2004), where $a_{ij} = P(X_{t+1} = s_j | X_t = s_i)$ represents the probability of transitioning from state s_i to state s_j.
- $\pi = [\pi_i]$ denotes the initial probability distribution, with $\pi_i = P(X_0 = s_i)$ and $\sum_i \pi_i = 1$.

If for any time index t and any sequence of past states, the process satisfies Revuz (2008)

$$P(X_{t+1} = s_j | X_t = s_i, X_{t-1}, \dots, X_0) = P(X_{t+1} = s_j | X_t = s_i) \tag{2}$$

then the process $\{X_t\}$ is said to follow the Markov property.

The *m-step transition probability* is defined as:

$$P_{ij}^{(m)} = P(X_{t+m} = s_j | X_t = s_i) \tag{3}$$

If the transition probabilities are independent of the time index t, i.e.,

$$P(X_{t+m} = s_j | X_t = s_i) = P_{ij}^{(m)} \tag{4}$$

the chain is said to be homogeneous. For $m = 1$, $P_{ij}^{(1)}$ is the one-step transition probability, and the m-step transition matrix Hou and Guo (2012) is given by:

$$P^{(m)} = [P_{ij}^{(m)}] \tag{5}$$

2.3.3. Dynamic Bayesian Network

A Dynamic Bayesian Network (DBN) extends the static Bayesian framework to time-dependent systems by incorporating temporal transitions between variables at successive time slices Murphy (2002). Essentially, it combines the representational power of Bayesian networks with the temporal dynamics of Markov models, thus enabling reasoning and learning from sequential data.

Since directly modeling the complete temporal evolution of all variables is computationally intractable, two simplifying assumptions are commonly adopted Shiguihara et al. (2021):

1. **Stationarity assumption:** The network topology and conditional dependencies remain invariant over time, i.e., for any time step t,

$$P(X_t | \mathrm{Pa}(X_t)) = P(X_{t+1} | \mathrm{Pa}(X_{t+1}))$$

2. **Markov assumption:** Given the current state X_t, the future state X_{t+1} is independent of all past states:

$$P(X_{t+1} | X_t, X_{t-1}, \dots, X_0) = P(X_{t+1} | X_t) \tag{6}$$

Based on these assumptions, a DBN can be formally defined as $(B_0, B_{\rightarrow})$, where B_0 represents the Bayesian structure at the initial time slice, and $B_{\rightarrow}$ denotes the inter-slice dependencies connecting variables across consecutive time slices Murphy (2002).

As illustrated in Figure **??**, intra-slice dependencies are represented by solid directed arcs, while inter-slice dependencies between successive time slices are represented by dashed arcs. The joint probability distribution of the DBN over all time slices can be written as:

$$P(X_{0:T}) = P(X_0) \prod_{t=1}^{T} P(X_t | X_{t-1}) \tag{7}$$

This recursive formulation enables efficient inference and temporal prediction in sequential decision and reliability modeling problems.

3. Methodology

This study integrates two complementary datasets to support both causal-prior construction and dynamic model calibration: (1) a large-scale set of incident reports from commercial NPPs in China collected between 2007 and 2021, and (2) a multimodal experimental dataset acquired from controlled simulator trials under different automation levels. Together, these sources provide the empirical foundation for deriving, validating, and contextualizing the proposed DBML-SA framework.

3.1. Overview of the Framework

The proposed research adopts a hybrid data-driven framework designed to quantitatively evaluate and predict operator SA levels in NPP control rooms. As illustrated in Figure 1, the framework is structured into four hierarchical layers, each corresponding to a distinct methodological stage—from data acquisition to predictive modeling and validation. Together, these layers establish a systematic workflow that integrates empirical evidence, probabilistic reasoning, and machine learning to support both interpretability and predictive capability.

The first layer focuses on event and experiment data collection. Historical operation event reports and controlled simulator experiments are used to obtain multi-source data describing PSFs, physiological indicators, and subjective SA measures. Event reports capture real plant experiences and error precursors, while simulator data provide controlled observations of dynamic operator behavior and physiological responses such as skin conductance and pupil variation.

The second layer performs statistical and causal modeling of SA factors. Through descriptive statistics, correlation analysis, and factor analysis, key PSFs influencing SA, such as training quality, teamwork, interface design, and task complexity, are identified and quantified. These analyses form the basis for constructing a data-driven causal structure that represents interdependencies among factors contributing to SA formation and degradation.

The third layer develops a DBN for temporal inference of SA reliability. The DBN extends conventional Bayesian reasoning by incorporating time-indexed nodes to capture the stochastic evolution of operator cognitive states. It enables forward and backward inference across time slices, allowing the estimation of SA degradation probability under different combinations of PSF states and dynamic variables.

The fourth layer introduces a machine learning prediction module to achieve automatic estimation of SA levels. Using the PSF data as inputs and subjective SART scores as training targets, a neural-network-based model learns nonlinear mappings between influencing factors and quantitative SA indicators. This component enhances predictive accuracy and supports real-time application, complementing the interpretability of the DBN with data-driven adaptability.

Collectively, these four layers constitute an integrated methodological framework that bridges empirical human performance data and probabilistic cognitive modeling. The approach enables both diagnostic analysis of causal mechanisms and predictive estimation of operator SA, providing a foundation for intelligent monitoring and decision support in digital main control rooms.

3.2. Data Sources and Preprocessing

The development of the proposed framework relied on both historical operation event data and structured expert evaluations to establish a quantitative foundation for modeling operator SA. A total of 212 domestic operation event reports collected from 2007 to 2021 were systematically reviewed to extract human-related causal information associated with SA failures. These reports cover a wide range of operational scenarios, including normal operations, transients, and abnormal events, and were selected based on their explicit reference to perception or comprehension errors in accordance with Endsley's three-level SA model.

From the content analysis of these reports, 11 PSFs influencing operator SA were identified in Table 1. The operational definitions and five-level rating criteria of these PSFs are summarized in Table 1, where a higher score indicates a more favorable condition.

To ensure objectivity and consistency, each event report was independently reviewed by five subject-matter experts from nuclear utilities and research institutes, all with more than ten years of experience in human-factor evaluation. Through consensus discussions, each PSF within an event was assigned a discrete rating from 1 to 5, representing levels ranging from "very poor" to "excellent." Events in which a specific PSF was not mentioned were coded as 0 (non-applicable). This process yielded a structured numerical dataset suitable for statistical and probabilistic modeling, and representative samples of the collected data are presented in Table 2.

Prior to analysis, the raw PSF ratings were normalized and standardized to remove scale effects across variables. Descriptive statistics were then computed to examine the central tendency and variability of each PSF. Correlation analysis indicated, for example, a significant positive relationship between stress and task complexity ($r = 0.463$, $p < 0.01$) and a negative correlation between stress and available time ($r = –0.252$, $p < 0.05$). These results highlight the interdependent nature of cognitive and contextual factors affecting SA.

Subsequently, factor analysis was performed to extract underlying latent constructs from the 11 PSFs, reducing dimensionality while preserving explanatory variance. Four principal factors were identified, representing (1) task and workload characteristics, (2) interface and automation quality, (3) procedural and environmental support, and (4)

Table 1
Definition of performance shaping factors (PSFs) and five-level scoring criteria

No.	PSF	Definition / Description	Scoring Criteria (1–5)[1]
1	Teamwork and communication	Effectiveness of coordination, information sharing, and mutual cross-checking among operators.	1 = Very poor (team conflict, no feedback); = Adequate (basic coordination); 5 = Excelle (cohesive, proactive communication).
2	Training level	Adequacy of operator knowledge, skill proficiency, and scenario familiarity.	1 = Inadequate (training gaps); 3 = Acceptab (basic competence); 5 = Highly proficient (fr quent simulation practice).
3	Procedure quality	Clarity, consistency, and accessibility of operating procedures.	1 = Ambiguous or incomplete; 3 = Usable b requires assistance; 5 = Clear and well-validate
4	Interface quality	Ergonomic quality and informativeness of the human–machine interface (HMI).	1 = Poor layout and information overload; 3 Acceptable clarity; 5 = Intuitive and integrate interface.
5	Task complexity	Degree of cognitive and procedural demand required to complete the task.	1 = Extremely complex; 3 = Moderate; 5 Simple and well-structured.
6	Automation level	Extent to which automation supports decision-making and reduces manual workload.	1 = Low automation (error-prone); 3 = Parti support; 5 = High automation with human ove sight.
7	Organizational factors	Effectiveness of management, safety culture, and organizational support.	1 = Weak management and poor culture; 3 Moderate; 5 = Strong safety-oriented organiz tion.
8	Available time	Time margin available for perception, comprehension, and action.	1 = Extremely tight; 3 = Adequate; 5 = Amp time for decision.
9	Work environment	Physical and ambient working conditions (noise, lighting, temperature, etc.).	1 = Unsuitable; 3 = Acceptable; 5 = Comfortab and well-controlled.
10	Attention level	Degree of concentration and situational focus maintained by the operator.	1 = Distracted or fatigued; 3 = Moderate focu 5 = Highly focused and alert.
11	Stress level	Psychological and physiological stress perceived during task performance.	1 = Extremely high stress; 3 = Moderate; 5 Calm and well-controlled.

team and organizational coordination. The resulting structure informed the causal relationships used in the Dynamic Bayesian Network (DBN) model developed in the next section.

Overall, this preprocessing stage transformed qualitative event narratives into a quantitative PSF dataset, enabling subsequent probabilistic reasoning and machine-learning prediction of operator SA levels.

3.3. Statistical and factor analysis

Following data normalization and preprocessing, a series of statistical analyses are performed to characterize the distributional properties, correlations, and latent structure of the identified PSFs. These analyses served as the foundation for developing the causal model of SA used in the subsequent DBN.

Descriptive statistics were first computed to examine the central tendency, variability, and overall quality of the collected PSF ratings. The majority of PSFs exhibited approximately normal distributions, indicating consistent expert judgment across the 212 analyzed events. The mean ratings of training, teamwork, and procedure quality were above 3.5, suggesting generally adequate human and organizational performance, whereas the mean scores of task complexity and stress level were comparatively lower, reflecting their significant challenge to operator SA during abnormal conditions. The overall standard deviations ranged from 0.72 to 1.12, implying moderate variability suitable for subsequent multivariate analysis.

Table 2
Data Collection of Situation Awareness-Related Operational Events and Influencing Factors

Event ID	Teamwork and Communication	Training Level	Procedure Quality	Human–Machine Interface	Task Complexity	Automation Level	Organizational Factors	Available Time	Work Environment	Attention Level	Stres Leve
LAo-1	2	1	1	1	0	3	2	0	0	0	0
ND-1	1	1	0	0	0	0	2	0	0	0	0
YJ-1	0	2	2	0	0	0	1	0	0	0	0
YJ-2	0	1	0	0	2	0	0	0	0	2	3
FQ-1	2	1	0	0	3	0	1	0	0	3	2
QS-1	1	1	0	2	0	0	2	0	0	1	0
DYW-1	0	2	0	2	3	0	1	0	0	1	3
DYW-2	0	2	1	0	2	0	2	0	0	0	2
LAo-2	0	0	0	2	0	0	2	0	0	1	0
…	…	…	…	…	…	…	…	…	…	…	…
…	…	…	…	…	…	…	…	…	…	…	…
FQ-10	1	2	0	0	2	0	2	0	2	2	0
QS-2	2	2	2	0	2	0	2	2	0	2	2

Pairwise pearson correlation coefficients were calculated to explore the interdependencies among the 11 PSFs. Several statistically significant relationships were identified, underscoring the multi-factor nature of cognitive performance. Notably, stress was found to be positively correlated with task complexity ($r = 0.463$, $p < 0.01$), indicating that complex operational demands tend to elevate operator stress levels and thereby influence SA. In contrast, available time was negatively correlated with stress ($r = –0.252$, $p < 0.05$), implying that compressed time margins exacerbate cognitive pressure. Furthermore, strong positive associations were observed between teamwork and communication, training level, and organizational factors, highlighting the reinforcing role of collaborative and cultural elements in sustaining operator awareness.

To reduce dimensionality and identify underlying latent constructs, an exploratory factor analysis was conducted using principal-component extraction with varimax rotation. The Kaiser–Meyer–Olkin (KMO) measure of sampling adequacy was 0.813, and Bartlett's test of sphericity was significant ($p < 0.001$), confirming the suitability of the dataset for factor analysis. Four principal components with eigenvalues greater than 1.0 were retained, collectively explaining 76.4 % of the total variance. These latent factors were interpreted as follows: (1) Cognitive and workload factor, encompassing task complexity, stress, and attention; (2) Procedural and training factor, including procedure quality and training level; (3) Environmental and interface factor, composed of interface quality, automation level, and work environment; and (4) Team and organizational factor, representing teamwork, communication, and organizational culture. Each factor exhibited strong internal consistency (Cronbach's $\alpha > 0.80$), supporting their reliability as aggregated constructs for causal modeling.

Based on the correlation patterns and extracted latent factors, a data-driven causal structure of operator SA was established, as depicted in Figure 2. The model conceptualizes SA as a function of four interacting dimensions: cognitive, procedural, environmental, and team-organizational, each influencing and being influenced by specific PSFs. Directed links between factors (e.g., from task complexity and stress to SA reliability) were derived from both statistical relationships and expert consensus, reflecting empirically supported causal pathways. This structure provides the backbone for the DBN model developed in Section 3.4, enabling temporal inference of SA degradation and recovery across operational sequences.

3.4. Dynamic Bayesian Network (DBN) Construction

To represent the probabilistic dependencies and temporal evolution of operator SA, a Dynamic Bayesian Network was developed based on the causal structure identified in the previous section. The DBN extends conventional BN reasoning by incorporating time-indexed nodes and transition probabilities, allowing the model to capture how SA reliability evolves under varying task and environmental conditions.

The DBN model comprises static nodes representing relatively stable PSFs and dynamic nodes corresponding to time-varying cognitive states. The static nodes include variables such as training level, teamwork, procedure quality,

interface design, task complexity, and automation level. These parameters reflect enduring contextual or organizational conditions that remain constant within a task episode.

In contrast, two dynamic nodes, stress and attention, were introduced to model operators' fluctuating physiological and cognitive states. These nodes interact bidirectionally with both the static PSFs and the output node SA reliability, representing the operator's overall cognitive readiness to perceive, comprehend, and project system status at each time slice. The resulting structure integrates both short-term cognitive variation and long-term contextual influence, providing a holistic probabilistic representation of SA dynamics.

The CPTs Rohmer (2020) defining relationships among the nodes were established through a combined analytic hierarchy process (AHP) Vaidya and Kumar (2006) and distance-based normalization procedure. Expert pairwise comparisons were first conducted to determine the relative importance of each PSF to SA reliability. These AHP-derived weights were then transformed into probability values using a relative distance index (R-index) method, which ensures consistency and scale normalization across heterogeneous variables. This hybrid elicitation approach integrates expert judgment with quantitative adjustment, mitigating subjectivity while maintaining interpretability. The final CPTs provide prior probabilities for each node and conditional dependencies among PSFs, stress, attention, and SA reliability.

To parameterize temporal transitions between successive states, the DBN incorporates physiological indicators collected from simulator-based experiments. Specifically:

- Stress transitions were derived from changes in electrodermal activity (EDA) Boucsein (2012), which reflects sympathetic nervous system arousal. The probability of stress escalation or reduction between time slices was computed by normalizing EDA variance within a moving time window.

- Attention transitions were modeled using pupil diameter variation, a validated correlate of cognitive workload and focus. The rate of pupil dilation was used to estimate attention fluctuation probabilities across time steps.

These physiological data streams enable the DBN to dynamically update SA reliability as operator stress and attention vary throughout a task sequence, thereby linking objective measurements to probabilistic reasoning. The complete DBN was implemented in the GeNIe modeling environment (developed by the Decision Systems Laboratory, University of Pittsburgh), which provides graphical interfaces for network design, CPT editing, and temporal inference. The model comprises two time slices (t and t+1), each containing identical node sets, with inter-slice arcs representing temporal transitions for dynamic nodes. Inference was performed using the Junction Tree algorithm, allowing both forward prediction of SA degradation and backward diagnosis of contributing factors.

The final DBN structure is shown in Figure 3, where directed edges illustrate the causal and temporal dependencies among static PSFs, dynamic cognitive states (stress and attention), and the output node representing operator SA reliability. This model serves as the probabilistic core of the hybrid framework, enabling dynamic, interpretable evaluation of SA during complex control room operations.

3.5. Experimental Validation

To validate the proposed DBN framework for quantitative SA evaluation, an experimental study was conducted using a steam generator tube rupture (SGTR) small-break scenario on a high-fidelity digital nuclear power plant simulator. The experiment aimed to provide empirical data for calibrating model parameters and verifying the consistency between predicted and observed SA levels under dynamic operational conditions.

Scenario Description. The SGTR scenario represents a typical abnormal event requiring rapid diagnosis and coordinated decision-making by operators. It involves the rupture of a single heat-transfer tube in the steam generator, leading to primary-to-secondary leakage and a gradual loss of reactor coolant inventory. The scenario was selected because it imposes substantial diagnostic uncertainty, multitasking, and cognitive load, all of which directly influence SA. The procedure included normal startup conditions, fault initiation, signal recognition, and recovery actions, lasting approximately 25 minutes in total.

Participants. A total of 41 participants took part in the experiment, comprising 33 licensed operators from nuclear utilities and 8 research subjects with extensive simulator training backgrounds. All participants had completed certified operational training programs and were familiar with digital main control room (DMCR) interfaces. Participants were divided into small operation teams of two to three persons to replicate realistic control-room collaboration. Prior to each trial, a standardized briefing was provided to ensure consistent understanding of task objectives and system configurations.

Table 3
Experimental variables and data sources for SGTR scenario validation

No.	Variable	Description / Measurement Method	Data Source
1	EDA	Mean skin conductance level and variance across time slices; indicator of physiological stress and arousal.	Wearable EDA sensor (Shimmer3 GSR+)
2	Pupil diameter variation	Average rate of pupil dilation and constriction; proxy for attention and cognitive workload.	Tobii Pro Fusion eye tracker
3	Gaze fixation duration	Mean fixation time and dispersion across interface elements; reflects information search efficiency.	Eye-tracking data synchronized with simulator logs
4	Procedure step count	Number of completed operating steps within each phase of the SGTR scenario.	Simulator operation log
5	Time pressure level	Ratio of available time to nominal procedure time; reflects urgency of task execution.	Scenario design parameters
6	Alarm frequency	Total number of visual or auditory alarms generated during each scenario stage.	Control system alarm record
7	SAGAT score	Correct response ratio to freeze-probe questions measuring perception, comprehension, and projection levels.	SAGAT questionnaire (two pause points)
8	SART score	Composite rating of attentional demand, information supply, and understanding level.	Post-scenario SART questionnaire
9	Team communication index	Number and duration of verbal exchanges among team members; indicator of collaborative coordination.	Audio and transcript coding
10	SA reliability (model output)	Posterior probability of maintaining correct SA at each time slice, calculated via DBN inference.	DBN model output

Data Collection. During the experiment, a multimodal dataset was collected combining physiological, behavioral, and subjective measures to support both model calibration and validation: (1) EDA: recorded via wearable sensors to quantify sympathetic arousal and stress variation; (2) Eye-tracking data: collected using head-mounted Tobii eye trackers to monitor gaze distribution, fixation duration, and pupil diameter as proxies for attention allocation; (3) Questionnaire assessments: operators completed both the SAGAT and the SART questionnaires for subjective SA evaluation.

To minimize interference with task performance, two pause points were predefined during the scenario, immediately after fault diagnosis and after corrective actions, to administer SAGAT queries and capture real-time SA states. SART questionnaires were completed post-trial to assess perceived attentional demand, information supply, and overall understanding. Physiological and behavioral data were continuously recorded throughout the experiment, synchronized with simulator logs.

Experimental Variables. The primary variables measured in the experiment included (1) physiological indicators (mean EDA, pupil dilation rate), (2) task and environmental parameters (procedure step count, time pressure level, and alarm frequency), and (3) subjective SA indices from SART and SAGAT results. These variables were aligned with corresponding nodes in the DBN model to enable quantitative comparison and dynamic updating of transition probabilities. A summary of the measured variables and their data sources is presented in Table 3.

3.6. Machine Learning Prediction Module

To complement the interpretability of the DBN with a data-driven predictive capability, a machine learning prediction module was developed to automatically estimate operator SA levels from quantifiable PSFs. The objective

of this module is to approximate the mapping between contextual and human factors and the subjective SART scores, thereby enabling real-time or near-real-time SA estimation.

Model Inputs and Outputs. The input layer of the model consisted of 11 PSFs, as defined in Table 1, encompassing both cognitive and environmental dimensions such as training, teamwork, procedure quality, interface design, task complexity, automation level, organizational factors, available time, work environment, attention, and stress. These variables were normalized to a [0, 1] range to eliminate scale bias and ensure numerical stability during training.

The output layer produced 10 quantitative SART items, representing the constituent dimensions of operator SA (e.g., attentional demand, information supply, understanding, and overall perceived awareness). Each output corresponds to an averaged SART rating derived from post-scenario questionnaires, enabling direct comparison between model predictions and subjective evaluations.

Network Architecture. A two-layer fully connected neural network (FCN) was implemented, as illustrated in Figure 3. The first hidden layer consisted of 64 neurons and the second of 32 neurons, both using rectified linear unit (ReLU) Agarap (2018) activation functions to introduce nonlinearity while maintaining computational efficiency. The output layer employed a linear activation function to generate continuous SART score predictions. The network parameters were initialized using Xavier uniform initialization to facilitate convergence and avoid vanishing gradients.

Regularization techniques—including dropout ($p = 0.2$) and L2 weight decay ($\lambda = 0.001$), were incorporated to mitigate overfitting and improve model generalization, given the relatively limited dataset size. The FCN was implemented in Python using the TensorFlow library.

Training and Validation. The network was trained for 20,000 iterations using the Adam optimization algorithm with an initial learning rate of 0.001 and mini-batch size of 8. The mean absolute percentage error (MAPE) was adopted as the primary loss metric due to its interpretability and robustness against outliers. To maximize model reliability under limited data, a leave-one-out cross-validation (LOOCV) scheme was employed: each sample was sequentially excluded as a test case while the remaining samples were used for training, ensuring unbiased performance evaluation.

During training, convergence was typically achieved after approximately 15,000 iterations, with validation MAPE stabilizing below 15%. The predicted SART profiles showed strong linear consistency with measured questionnaire scores ($R^2 > 0.82$, $p < 0.01$), confirming the feasibility of estimating SA levels from PSF inputs alone. These results demonstrate the model's capacity to capture nonlinear interactions among influencing factors and to approximate subjective awareness states quantitatively.

Model Integration. The FCN-based prediction module was integrated with the probabilistic DBN framework to form a hybrid SA evaluation system. While the DBN provides causal interpretability and diagnostic reasoning, the neural network enables continuous, data-driven estimation of SA with minimal human intervention. This complementary architecture supports scalable deployment for real-time monitoring and adaptive operator support in digital main control rooms.

4. Results and Analysis

4.1. DBN Temporal Inference

The DBN constructed in Section 3.4 was applied to infer the temporal evolution of operator SA reliability during the SGTR small-break scenario. The model was executed over ten discrete time slices (t_0–t_9), corresponding to key phases of the operating procedure, from initial fault occurrence through system diagnosis and recovery. Each time slice represents a transition state in which dynamic variables (stress and attention) update their probabilities based on physiological inputs, while static PSFs maintain contextual consistency.

The inference results reveal a gradual decline in SA reliability as the scenario progressed, reflecting the accumulation of cognitive workload and information processing demands under fault conditions. The posterior probability of maintaining adequate SA decreased from 0.778 at t_0 to 0.762 at t_9, representing a 2.1 % reduction across the operational sequence. Although this decline appears modest in magnitude, it is consistent with expected cognitive fatigue effects observed in time-critical control tasks, where continuous monitoring and diagnostic reasoning incrementally tax attentional resources.

The temporal pattern further indicates that SA reliability remained relatively stable during the early diagnostic phase (t_0–t_3) but exhibited a sharper decrease after the fault recognition stage (t_4–t_6), coinciding with the peak of task complexity and alarm density (Figure 5). In later stages (t_7–t_9), the probability curve reached a steady plateau as the operators executed corrective procedures and system parameters began to stabilize. These dynamics confirm that the

Table 4
Percentage Change in Probabilities of Variable Factors

Time Slice	Variable State	Available Time	Procedure Quality	Task Complexity	Training Level	Teamwork Level	HMI	A Le
	Prior Probability	0.14	0.05	0.15	0.04	0.09	0.08	0.
t_2 Slice	Posterior Probability	0.18	0.06	0.19	0.11	0.11	0.09	0.
	Change Rate / %	28.6%	20.0%	26.6%	175.0%	22.2%	12.5%	0.

DBN effectively captures both transient fluctuations and long-term trends in cognitive performance. The percentage change in probabilities of variable factors is shown in Table 4.

Overall, the temporal inference results demonstrate the DBN's capability to integrate time-dependent physiological evidence with contextual PSFs to produce a continuous, probabilistic profile of SA reliability. This enables quantitative tracking of operator cognitive state transitions throughout complex event sequences, providing valuable insights for real-time monitoring and human reliability evaluation in digital control room environments.

4.2. Diagnostic Reasoning and Sensitivity Analysis

Beyond temporal inference, the DBN framework was further utilized to perform diagnostic reasoning and sensitivity analysis, enabling the identification of key factors that most strongly influence operator SA. Diagnostic reasoning within the DBN provides a backward-inference capability: when a target state (e.g., SA failure) is observed, the model estimates the posterior probabilities of contributing PSFs, thereby revealing the relative influence of human, procedural, and environmental conditions.

When the SA failure event was defined as a posterior state with $P_{failure} = 1$, the DBN identified training quality and stress variation as the two dominant contributors to SA degradation. The posterior probability of low training level increased by 18.7%, while that of high stress level increased by 16.4 % relative to their baseline priors. These findings suggest that inadequate training exacerbates diagnostic uncertainty and error susceptibility under high workload conditions, while stress fluctuations amplify cognitive instability and attentional lapses during complex task execution.

In contrast, other PSFs such as teamwork effectiveness, interface quality, and available time exhibited smaller posterior deviations (typically below 7 %), indicating secondary but non-negligible contributions to overall SA reliability. This hierarchical attribution pattern aligns with empirical observations from simulator experiments, where both cognitive preparedness (training) and psychophysiological state (stress) were found to be decisive determinants of operator awareness and decision accuracy.

A subsequent global sensitivity analysis was conducted to quantify the responsiveness of the DBN output (SA reliability) to perturbations in each input node. Results confirmed high sensitivity (>10 % variation) to both training and stress nodes, moderate sensitivity (5–10 %) to attention and task complexity, and lower sensitivity (<5 %) to structural factors such as interface quality and automation level. This demonstrates that SA reliability in dynamic operational contexts is more susceptible to human cognitive and emotional factors than to environmental or procedural variations.

Overall, the diagnostic and sensitivity analyses validate the DBN's capacity for interpretable causal reasoning, allowing quantitative identification of key contributors to SA degradation. Such insights are critical for targeted operator training, interface optimization, and workload management strategies aimed at mitigating human error in digital control room operations.

4.3. Validation Against Subjective Assessments

To examine the validity and practical reliability of the proposed DBN framework, its quantitative outputs were compared with subjective SA assessments obtained from the experimental study described in Section 3.5. Two well-established methods, the SAGAT and the SART, were used as benchmark references for validation.

Comparison with SAGAT Result. The SA reliability values inferred from the DBN were first compared with the SAGAT-based SA scores measured at the two pause points during the SGTR scenario. The comparison revealed a strong consistency between model predictions and empirical SAGAT data, with an average absolute difference below 5.0 % across all time slices. The temporal trends of both metrics exhibited near-identical profiles: high SA reliability

Table 5
Posterior probability changes across variables under SA failure conditions

No.	Variable (Node)	Description / Interpretation	Posterior Change (%)
1	Training quality	Level of operator knowledge and skill proficiency; insufficient training increases diagnostic errors under stress.	+18.7
2	Stress variation	Degree of psychophysiological arousal inferred from EDA signals; elevated stress reduces cognitive stability.	+16.4
3	Attention level	Probability of maintaining sustained focus on key interface indicators.	+9.3
4	Task complexity	Cognitive and procedural demand associated with fault diagnosis and recovery.	+7.8
5	Teamwork and communication	Effectiveness of coordination and cross-checking among operators.	+6.5
6	Interface quality	Ergonomic clarity and visual integration of control displays.	+4.8
7	Available time	Margin between allocated and required time for correct action execution.	+4.1
8	Procedure quality	Clarity and applicability of operating procedures under abnormal conditions.	+3.7
9	Automation level	Degree of automatic support reducing operator workload.	+3.2
10	Organizational factors	Strength of safety culture and managerial oversight supporting operator performance.	+2.9

Table 6
One-Way Analysis of Variance (ANOVA)

Model	Sum of Squares	df	Mean Square	F	Significance
Between Groups	0.073	9	0.008	1.443	0.385
Within Groups	0.022	4	0.006		
Total	0.095	13			

during the initial diagnostic stages followed by a slight decline as task complexity and cognitive demand increased. This agreement confirms that the DBN successfully captures the dynamic characteristics of operator cognition that are otherwise only observable through intrusive experimental methods such as SAGAT probing.

Comparison with SART Results. A further cross-validation was performed against the post-scenario SART questionnaire scores, which represent operators' perceived understanding, information supply, and attentional demand. Statistical analysis using a one-way analysis of variance (ANOVA) Quirk (2012) indicated no significant difference between the DBN-predicted SA reliability and the subjective SART composite scores ($p = 0.385 > 0.05$). This result in Table 6 demonstrates that the probabilistic estimates produced by the DBN are statistically equivalent to operators' self-reported awareness levels, despite being derived entirely from objective PSF and physiological data.

Validation Summary. Taken together, the validation results substantiate the credibility and accuracy of the proposed framework. The DBN not only reproduces the temporal patterns captured by SAGAT but also aligns closely with subjective perceptions reflected in SART. Hence, the model provides a viable quantitative alternative to traditional, labor-intensive SA measurement techniques, supporting continuous, data-driven evaluation of cognitive reliability in digital control room environments.

Table 7
Comparison of DBN-predicted results and questionnaire-based SA measurements

No.	Assessment Point	DBN-Predicted SA Reliability	SAGAT-Measured SA Score	Absolute Difference (%)	SART Composite Score
1	Diagnostic phase (t_3)	0.776	0.791	1.9	0.774
2	Fault recognition (t_5)	0.769	0.785	2.0	0.763
3	Recovery initiation (t_7)	0.764	0.781	2.2	0.758
4	System stabilization (t_9)	0.762	0.778	2.1	0.756
		Mean values		**< 5.0**	

Note: DBN = Dynamic Bayesian Network; SAGAT = Situation Awareness Global Assessment Technique; SART = Situation Awareness Rating Technique. No significant difference was observed between DBN-predicted and SART-measured SA scores based on one-way ANOVA (*p* = 0.385 > 0.05).

4.4. Machine Learning Prediction

The performance of the fully connected neural network (FCN) module Dai, Li, He and Sun (2016) described in Section 3.6 was evaluated using both instantaneous and temporal prediction tasks to assess its capability in estimating operator SA from PSFs. The trained model was tested using the experimental dataset collected from the SGTR scenario, with SART questionnaire scores serving as ground truth labels for comparison.

Instantaneous Prediction Performance. For instantaneous prediction, where each observation was treated independently, the FCN achieved a mean absolute percentage error (MAPE) of 14.3 % across all test samples (Figure 6). The predicted SA scores closely followed the measured SART results, demonstrating the model's ability to approximate nonlinear relationships between PSFs and operator cognitive states. The regression fit between predicted and measured SART scores yielded a determination coefficient of $R^2 = 0.83$ ($p < 0.01$), confirming strong agreement and robust predictive capability under static conditions.

Temporal Prediction Performance. When extended to temporal sequences, where time-dependent PSF variations were aggregated across multiple task phases (t_0–t_9), the model maintained satisfactory accuracy with a MAPE of 16.5 %. Although slightly higher than in the instantaneous case, this result indicates the model's resilience in handling dynamic input fluctuations and its ability to generalize over time-varying cognitive and operational contexts. The observed deviation primarily stems from transient spikes in stress and attention metrics during high-load stages of the SGTR scenario.

The resulting outputs are shown in Figures 7 (a) and (b), where the MAPE of the predicted dynamic factors and dynamic SART scores were approximately 45.1% and 16.5%, respectively. After rounding to the nearest integer, the MAPE values were 44.5% and 17.3%, showing negligible difference from the unrounded results. Compared with the momentary prediction model, it can be observed that the temporal inference uncertainty substantially affects the predictive performance of the period-based model.

Consistency Across SART Dimensions. A detailed comparison across the four SART dimensions—comprehension, information supply, attentional demand, and overall SA—showed consistent trends between the model predictions and subjective ratings, with all relative errors remaining below 20%. Further comparative analyses of the overall comprehension level, overall demand level, overall supply level, and overall situation awareness level are presented in Figure 8. From the perspective of trend variation, the predicted results for overall comprehension, overall supply, and overall SA exhibit strong consistency with the subjective trends. In terms of prediction accuracy, the mean absolute percentage errors (MAPE) of the predicted values were 1.6 %, 19.6%, 15.9%, and 13.8%, respectively. After rounding, the MAPE values were 1.3%, 21.2%, 15.4%, and 13.7%, respectively. Although the differences before and after rounding were negligible, all prediction errors remained within acceptable limits, indicating that the proposed model can effectively substitute the SART questionnaire for evaluating situation awareness levels.

Validation Summary. Overall, the FCN-based prediction module demonstrated strong agreement with subjective SART assessments, both in instantaneous and temporal prediction modes. The results confirm that SA can be quantitatively inferred from PSF-based indicators with acceptable precision and stability, without the need for intrusive measurement procedures. As illustrated in Figure 8, the predicted SART scores exhibit parallel trajectories to the

measured values across all experimental stages, validating the model's applicability for real-time monitoring and cognitive performance prediction in digital control room environments.

5. Discussion

5.1. Theoretical Implications

The proposed DBN framework advances the theoretical understanding of operator SA within the broader context of HRA. By explicitly modeling the multi-factor causal pathways that govern SA formation and degradation, the framework provides a quantitative means to represent the complex interactions among PSFs, cognitive states, and behavioral outcomes. Unlike conventional static probability models that treat human error as an isolated event, the DBN captures time-dependent dependencies and recursive feedback between cognitive, procedural, and environmental variables, thereby formalizing SA as a dynamic and probabilistic construct.

From a theoretical standpoint, this approach bridges the gap between descriptive cognitive theories of SA, traditionally based on qualitative observations, and analytically tractable reliability models. The inclusion of causal reasoning structures enables forward inference (predicting SA reliability given PSF conditions) and backward diagnosis (identifying root causes of SA failure), offering a unified probabilistic interpretation of operator cognition under uncertainty. Such capability extends the classical HRA paradigm from static error quantification to dynamic cognitive reliability modeling, where operator performance is viewed as an evolving function of internal and external factors.

Furthermore, the integration of physiological indicators, such as electrodermal activity and pupil dilation, enhances the ecological validity and realism of the model. These indicators provide measurable evidence linking psychophysiological responses to cognitive workload and attentional control, allowing the DBN to update belief states continuously in accordance with observable operator behavior. This data-driven linkage between cognitive state variables and physiological evidence establishes a theoretical foundation for human digital twin modeling in nuclear operations, supporting future research on adaptive, evidence-based HRA frameworks.

In summary, the DBN framework contributes to the theoretical evolution of HRA by introducing a causal, time-resolved, and physiologically informed representation of situation awareness. It thus redefines SA not merely as a subjective or post-hoc construct, but as a dynamic reliability parameter amenable to probabilistic reasoning and empirical validation.

5.2. Practical Implications

Beyond its theoretical contributions, the proposed DBN–based framework offers substantial practical value for digital nuclear power plant operations. By combining probabilistic reasoning with data-driven prediction, the framework can be seamlessly embedded into digital main control room monitoring systems to support intelligent human–system interaction and enhance operational safety.

In practice, the model enables real-time tracking of operator SA through continuous inference of cognitive reliability based on measurable PSFs and physiological indicators. As the DBN dynamically updates its belief states with incoming data, such as changes in stress or attention, it can provide operators and supervisors with instantaneous feedback on cognitive performance, including early signs of overload, distraction, or misperception. This capability allows the system to issue early warnings of SA degradation, enabling timely intervention through adaptive task allocation, procedural assistance, or automation support before performance loss leads to human error.

From a system-integration perspective, the framework is compatible with existing plant information and alarm management architectures. Its modular design allows deployment as part of an operator support system or within a human reliability monitoring module in advanced control platforms. The probabilistic reasoning outputs can be visualized as dynamic SA indicators or risk dashboards, facilitating supervisory decision-making and real-time situational oversight.

Moreover, the framework supports data-driven human factors engineering by providing quantitative feedback for training program design, interface optimization, and workload management. Insights derived from sensitivity and diagnostic analyses can guide targeted improvements in operator training and procedural standardization, reinforcing organizational resilience against cognitive failure.

In summary, the integration of the proposed framework into digital control environments provides a pathway toward intelligent, adaptive, and human-centered safety monitoring. It bridges human reliability analysis with operational decision support, enabling continuous assessment of cognitive performance and proactive mitigation of human error in complex nuclear systems.

Table 8
Comparison of machine learning models for SA regression prediction

Model	Type	Input Features	R^2	MAPE (%)	Key Advantage
FCN (Instantaneous)	Static	11 PSFs	**0.83**	14.3	Strong nonlinear mapping accuracy
Multi-Factor FCN	Static (expanded)	12 PSFs + embedding	0.62	**9.47**	Best overall performance
LSTM	Temporal	12 PSFs + embedding (sequence)	0.34	14.83	Captures temporal dynamics
				Highest accuracy: Multi-Factor FCN (MAPE = 9.47%)	

Note: FCN = Fully Connected Neural Network; LSTM = Long Short-Term Memory; PSFs = Performance Shaping Factors; SA = Situation Awareness; MAPE = Mean Absolute Percentage Error. All models were trained using Adam optimizer (learning rate = 0.001) and evaluated on independent test sets.

5.3. Comparative Performance of Machine Learning–Based SA Regression Models

To further interpret the predictive mechanisms and practical implications of the proposed framework, three machine learning models—a feedforward neural network (FCN), an extended multi-factor FCN, and an LSTM-based temporal regression model—were comparatively analyzed. These models were designed to progressively capture static and dynamic dependencies between multidimensional performance shaping factors (PSFs) and subjective situation awareness (SA) scores.

Static FCN Models. The baseline FCN, trained on instantaneous PSF data from the SGTR simulator experiments, achieved a mean absolute percentage error (MAPE) of 14.3

Temporal Model. To explore dynamic cognitive variations, a two-layer LSTM model was trained using sequential PSF data spanning ten task phases (t_0–t_9). The model achieved a MAPE of 14.83

Cross-Model Insights. A comparative summary (Table 8) reveals that the multi-factor FCN achieved the best overall performance, striking a practical balance between accuracy, interpretability, and data requirements. The instantaneous FCN reached the highest determination coefficient ($R^2 = 0.83$) under controlled conditions, while the LSTM offered improved temporal generalization at the expense of reduced explanatory power. These trade-offs reflect the intrinsic differences between static and dynamic modeling paradigms: static models excel with limited data and clearer factor–outcome relationships, whereas temporal models require extensive sequences to effectively learn time-varying cognitive processes.

Implications. These results collectively verify the feasibility of machine learning–based quantitative estimation of operator SA from PSF data. The static FCN models, particularly the multi-factor variant, demonstrate strong reliability and interpretability under limited data conditions—attributes crucial for human reliability analysis in nuclear operations. Temporal extensions such as the LSTM offer an important complement by enabling continuous monitoring, yet their accuracy remains constrained by sample size and measurement noise. Overall, the FCN architecture provides a robust and explainable foundation for integrating data-driven cognitive estimation into dynamic Bayesian or hybrid probabilistic frameworks such as DBML-SA.

Among all evaluated architectures, the FCN exhibited the most balanced combination of accuracy, robustness, and interpretability, making it the preferred model for quantitative SA estimation. Trained on instantaneous PSF data from SGTR simulator experiments, the FCN achieved a MAPE of 14.3% and $R^2 = 0.83$ ($p < 0.01$), indicating strong consistency with measured SART scores (Figure 6). Its superior performance stems from efficiently capturing the nonlinear mapping between PSFs and cognitive states without relying on large sequential datasets, thereby converging faster and generalizing better under limited samples, an inherent constraint in human reliability research. The FCN's transparent input–output relationships facilitate sensitivity analysis, clarifying how training, procedure quality, interface design, and stress contribute to SA. Owing to its structural simplicity and reproducibility, the FCN can be readily integrated into the DBML-SA framework as a stable momentary inference module, providing real-time cognitive estimates and a scalable foundation for intelligent human–machine reliability assessment.

6. Conclusions and Future Work

This study developed a hybrid dynamic Bayesian–machine learning framework (DBML-SA) for quantitative evaluation and prediction of operator situation awareness in nuclear power plant control rooms. By integrating probabilistic reasoning with data-driven prediction, the proposed model captures the multifactorial and time-dependent characteristics of operator cognition and reliability. The DBN component provides interpretable causal reasoning among performance-shaping factors, effectively modeling the causal relations and temporal evolution of SA degradation, while the neural network module enables continuous prediction of SA levels from quantifiable PSF inputs. Together, these elements constitute a coherent analytical framework that bridges subjective and objective methods for cognitive performance assessment.

Validation results demonstrated strong agreement between the model predictions and traditional SA evaluation techniques. The DBN-predicted SA reliability values showed high consistency with SAGAT-derived measurements, with an average deviation below 5%. Statistical comparison with post-scenario SART scores revealed no significant difference ($p = 0.385 > 0.05$), confirming the robustness and credibility of the proposed approach. These findings indicate that the hybrid framework can quantitatively and reliably represent dynamic operator cognition without the need for intrusive or subjective assessment procedures. The results provide both theoretical and practical foundations for real-time human reliability monitoring in next-generation digital main control rooms.

Nevertheless, several limitations should be acknowledged. The relatively limited dataset may introduce overfitting risks in the neural network training process, thereby constraining the model's generalization capability. Moreover, the current version of the framework does not incorporate task semantic encoding, which restricts its adaptability to unseen operational scenarios or procedures with distinct contextual structures. Addressing these issues will be essential for improving the universality and interpretability of the model.

Future research will focus on expanding the framework through the integration of multimodal data sources, including voice communication, behavioral logs, and gaze-tracking patterns, to enrich cognitive state characterization. The introduction of knowledge graph–based semantic encoding will further enhance contextual understanding and enable transfer learning across different tasks. In addition, the implementation of real-time visualization modules for SA dynamics will support interactive monitoring and adaptive operator assistance in complex control environments. These advancements are expected to evolve the present framework into an intelligent, context-aware human reliability analysis system, capable of supporting predictive safety management in future nuclear power plants.

CRediT authorship contribution statement

Shuai Chen: Conceptualization, Methodology, Software, Formal analysis, Data Curation, Visualization, Validation, Writing- Original draft preparation.. **Huiqiao Jia:** Validation, Writing- Original draft preparation.. **Tao Qing:** Validation, Writing- Original draft preparation.. **Li Zhang:** Validation, Writing- Original draft preparation.. **Xingyu Xiao:** Writing- Original draft preparation..

A. Factors Influencing Situation Awareness and Scoring Criteria

B. SAGAT Questionnaire

References

Agarap, A.F., 2018. Deep learning using rectified linear units (relu). arXiv preprint arXiv:1803.08375 .

Alberti, A.L., Agarwal, V., Gutowska, I., Palmer, C.J., de Oliveira, C.R., 2023. Automation levels for nuclear reactor operations: A revised perspective. Progress in Nuclear Energy 157, 104559.

Boring, R.L., Joe, J.C., Mandelli, D., 2015. Human performance modeling for dynamic human reliability analysis, in: International Conference on Digital Human Modeling and Applications in Health, Safety, Ergonomics and Risk Management, Springer. pp. 223–234.

Boucsein, W., 2012. Electrodermal activity. Springer science & business media.

Chung, K.L., 1967. Markov chains. Springer-Verlag, New York .

Dai, J., Li, Y., He, K., Sun, J., 2016. R-fcn: Object detection via region-based fully convolutional networks. Advances in neural information processing systems 29.

De Ambroggi, M., Trucco, P., 2011. Modelling and assessment of dependent performance shaping factors through analytic network process. Reliability Engineering & System Safety 96, 849–860.

Deng, Q., Xiao, X., Zhu, L., Cao, X., Liu, K., Zhang, H., Huang, L., Yu, F., Jiang, H., Liu, Y., 2023. A national risk analysis model (nram) for the assessment of covid-19 epidemic. Risk Analysis 43, 1946–1961.

Eddy, S.R., 2004. What is a hidden markov model? Nature biotechnology 22, 1315–1316.

Table 9
Factors Influencing Situation Awareness and Scoring Criteria

Factor	Description	1	2	3	4	5	Typical indications in reports or required conditions
Team Communication and Cooperation	Cooperation level	Poor	Fairly poor	Nominal	Good	Excellent	"Unexpected operation not reported to supervisor"; "No pre-operation communication"; "Information not transmitted"; "Premature closure of communication"; "Lack of supervision"; "Communication error during shift change"; "Handover failed to mention xxx"; "Lack of communication"; "Forgot to check handover info"; "Information not effectively conveyed"; "Insufficient communication"; "Unclear equipment status"; "Three-step communication not performed"; "Key points emphasized"; "Feedback confirmed"; "Comprehensive pre-job meeting held."
Training Level	Training quality	Poor	Fairly poor	Nominal	Good	Excellent	"No training conducted"; "Command not canceled in time"; "Failed to confirm/discover key parameter"; "Improper operation"; "Cognitive bias"; "Inadequate understanding of system principles"; "Skill deficiency"; "Deviation in comprehension"; "Procedure not reviewed"; "Alarm not verified."
Procedure Quality	Procedure completeness	Poor	Fairly poor	Average	Fairly good	Excellent	"No applicable operation procedure"; "No risk warning"; "Human-factor trap exists"; "Procedure outdated"; "Incomplete or ambiguous descriptions"; "Missing check step"; "Inadequate risk warning."
Human–Machine Interface	Interface usability	Poor	Fairly poor	Average	Fairly good	Excellent	"No alarm reminder for xxx"; "Key parameter unavailable"; "Curve display lost"; "Limited info presentation"; "No confirmation required"; "Alarm interference"; "Unclear labels."
Task Complexity	Complexity level	Very simple	Fairly simple	Average	Fairly complex	Highly complex	"Reactor/plant state complex."
Automation Level	System automation	Low	Fairly low	Average	Fairly high	High	"Online monitoring exists but requires manual confirmation."
Organizational Factors	Management quality	Poor	Fairly poor	Average	Fairly good	Excellent	"Procedure not followed"; "Risk control barrier failure"; "Human error prevention tools not used"; "Low standards"; "Lack of attention"; "No pre-job meeting"; "Inadequate planning"; "Poor communication"; "Overconfidence"; "Inadequate supervision."
Available Time	Time sufficiency	Insufficient	Tight	Nominal	Fairly sufficient	Sufficient	"Insufficient intervention time"; "Tight operation schedule."
Work Environment	Environmental quality	Poor	Fairly poor	Average	Fairly good	Excellent	—
Attention Level	Attention status	Distracted	Fairly distracted	Average	Fairly focused	Focused	"Failed to notice abnormal signals"; "Busy with other tasks"; "Neglect"; "Concurrent operations"; "Distracted by alarms or calls."
Stress Level	Stress intensity	High	Fairly high	Nominal	Low	Very low/None	—

Endsley, M.R., 1988. Situation awareness global assessment technique (sagat), in: Proceedings of the IEEE 1988 national aerospace and electronics conference, IEEE. pp. 789–795.

Endsley, M.R., 2021. Situation awareness. Handbook of human factors and ergonomics , 434–455.

Endsley, M.R., Garland, D.J., et al., 2000. Theoretical underpinnings of situation awareness: A critical review. Situation awareness analysis and measurement 1, 3–21.

Gertman, D., Blackman, H., Marble, J., Byers, J., Smith, C., et al., 2005. The spar-h human reliability analysis method. US Nuclear Regulatory Commission 230, 35.

Gorman, J.C., Cooke, N.J., Winner, J.L., 2017. Measuring team situation awareness in decentralized command and control environments, in: Situational awareness. Routledge, pp. 183–196.

Graves, A., 2012. Long short-term memory. Supervised sequence labelling with recurrent neural networks , 37–45.

Hou, Z., Guo, Q., 2012. Homogeneous denumerable Markov processes. Springer Science & Business Media.

Kasneci, E., Kübler, T., Broelemann, K., Kasneci, G., 2017. Aggregating physiological and eye tracking signals to predict perception in the absence of ground truth. Computers in Human Behavior 68, 450–455.

Kim, Y., Park, J., Jung, W., Jang, I., Seong, P.H., 2015. A statistical approach to estimating effects of performance shaping factors on human error probabilities of soft controls. Reliability Engineering & System Safety 142, 378–387.

Kirwan, B., 1983. Technique for human error rate prediction (therp). by Swain and Guttman .

Koller, D., Friedman, N., 2009. Probabilistic graphical models: principles and techniques. MIT press.

Larouzee, J., Le Coze, J.C., 2020. Good and bad reasons: The swiss cheese model and its critics. Safety science 126, 104660.

Li, P.c., Zhang, L., Dai, L.c., Li, X.F., 2017. Study on operator's sa reliability in digital npps. part 1: The analysis method of operator's errors of situation awareness. Annals of Nuclear Energy 102, 168–178.

Li, Q., Liang, Y., Wang, Z., Luo, L., Chen, X., Liao, M., Wei, F., Deng, Y., Xu, S., Zhang, Y., et al., 2024. Cogact: A foundational vision-language-action model for synergizing cognition and action in robotic manipulation. arXiv preprint arXiv:2411.19650 .

Logothetis, N.K., Pauls, J., 1995. Psychophysical and physiological evidence for viewer-centered object representations in the primate. Cerebral cortex 5, 270–288.

Murphy, K.P., 2002. Dynamic bayesian networks: representation, inference and learning. University of California, Berkeley.

Nagarajan, R., Scutari, M., Lèbre, S., 2013. Bayesian networks in r. Springer 122, 125–127.

Osman, M., 2010. Controlling uncertainty: a review of human behavior in complex dynamic environments. Psychological bulletin 136, 65.

Parasuraman, R., Sheridan, T.B., Wickens, C.D., 2008. Situation awareness, mental workload, and trust in automation: Viable, empirically supported cognitive engineering constructs. Journal of cognitive engineering and decision making 2, 140–160.

Park, J., Jung, W., Kim, J., 2020. Inter-relationships between performance shaping factors for human reliability analysis of nuclear power plants. Nuclear Engineering and Technology 52, 87–100.

Quirk, T.J., 2012. One-way analysis of variance (anova), in: Excel 2007 for educational and psychological statistics: A guide to solving practical problems. Springer, pp. 163–179.

Ramsey, N.F., Jansma, J.M., Jager, G., Van Raalten, T., Kahn, R., 2004. Neurophysiological factors in human information processing capacity. Brain 127, 517–525.

Revuz, D., 2008. Markov chains. volume 11. Elsevier.

Rohmer, J., 2020. Uncertainties in conditional probability tables of discrete bayesian belief networks: A comprehensive review. Engineering Applications of Artificial Intelligence 88, 103384.

Shiguihara, P., Lopes, A.D.A., Mauricio, D., 2021. Dynamic bayesian network modeling, learning, and inference: A survey. IEEE Access 9, 117639–117648.

Taylor, R.M., 2017. Situational awareness rating technique (sart): The development of a tool for aircrew systems design, in: Situational awareness. Routledge, pp. 111–128.

Vaidya, O.S., Kumar, S., 2006. Analytic hierarchy process: An overview of applications. European Journal of operational research 169, 1–29.

Xiao, X., Chen, P., Qi, B., Zhao, H., Liang, J., Tong, J., Wang, H., 2025a. Krail: A knowledge-driven framework for human reliability analysis integrating idheas-data and large language models. Reliability Engineering & System Safety , 111585.

Xiao, X., Liang, J., Tong, J., Wang, H., 2024. Emergency decision support techniques for nuclear power plants: Current state, challenges, and future trends. Energies 17, 2439.

Xiao, X., Qi, B., Liang, J., Tong, J., Deng, Q., Chen, P., 2023. Enhancing loca breach size diagnosis with fundamental deep learning models and optimized dataset construction. Energies 17, 159.

Xiao, X., Qi, B., Liu, S., Chen, P., Liang, J., Tong, J., Wang, H., 2025b. A dynamic risk-informed framework for emergency human error prevention in high-risk industries: A nuclear power plant case study. Reliability Engineering & System Safety 261, 111080.

Xiao, X., Zhu, H., Liang, J., Tong, J., Wang, H., 2025c. A comprehensive review of human error in risk-informed decision making: Integrating human reliability assessment, artificial intelligence, and human performance models. arXiv preprint arXiv:2507.01017 .

Zhang, J., Yang, X., Yin, Z., Liu, P., . Study and application of idheas-eca reliability analysis method for nuclear power, in: Man-Machine-Environment System Engineering: Proceedings of the 25th Conference on MMESE, Volume 2, Springer Nature. p. 246.

Zhang, T., Horigome, M., 2001. Availability and reliability of system with dependent components and time-varying failure and repair rates. IEEE Transactions on reliability 50, 151–158.

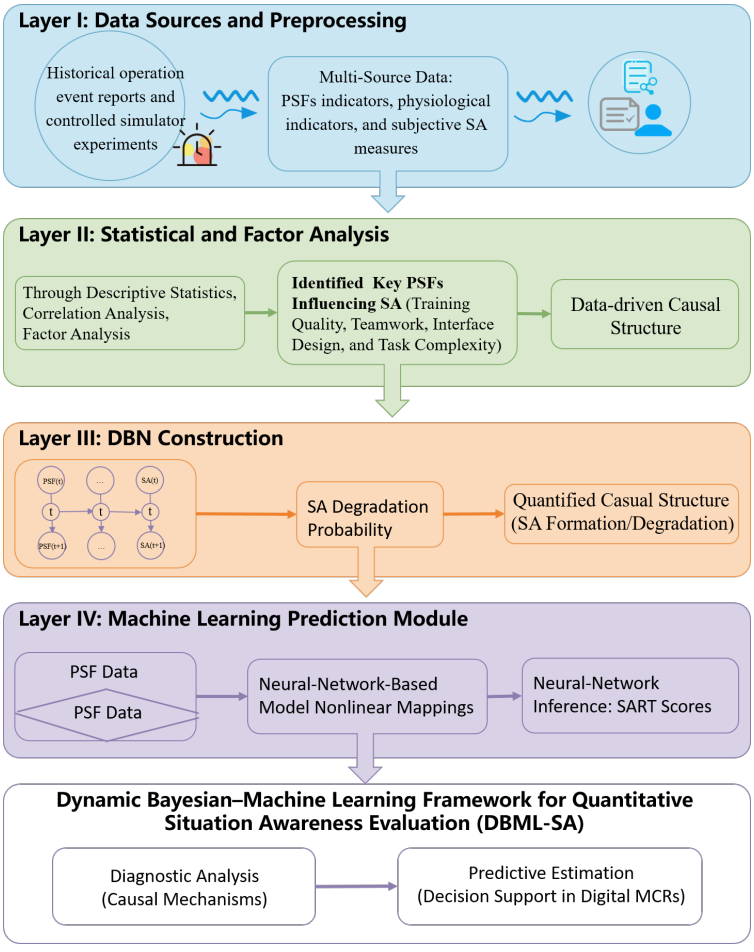

Figure 1: Workflow of the proposed Dynamic Bayesian–Machine Learning Framework (DBML-SA) for quantitative evaluation and prediction of operator situation awareness.

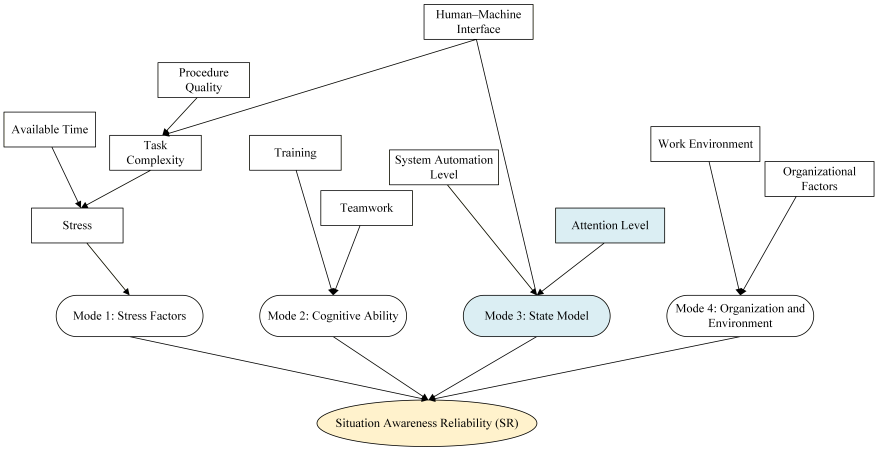

Figure 2: Causal model of situation awareness factors.

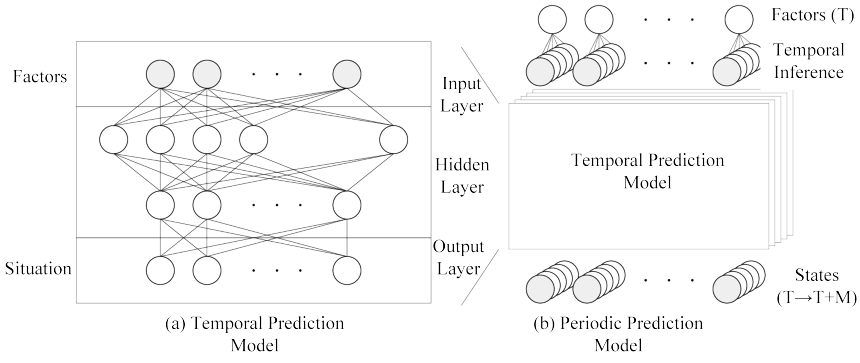

Figure 3: Neural network architecture for automatic prediction of SART scores.

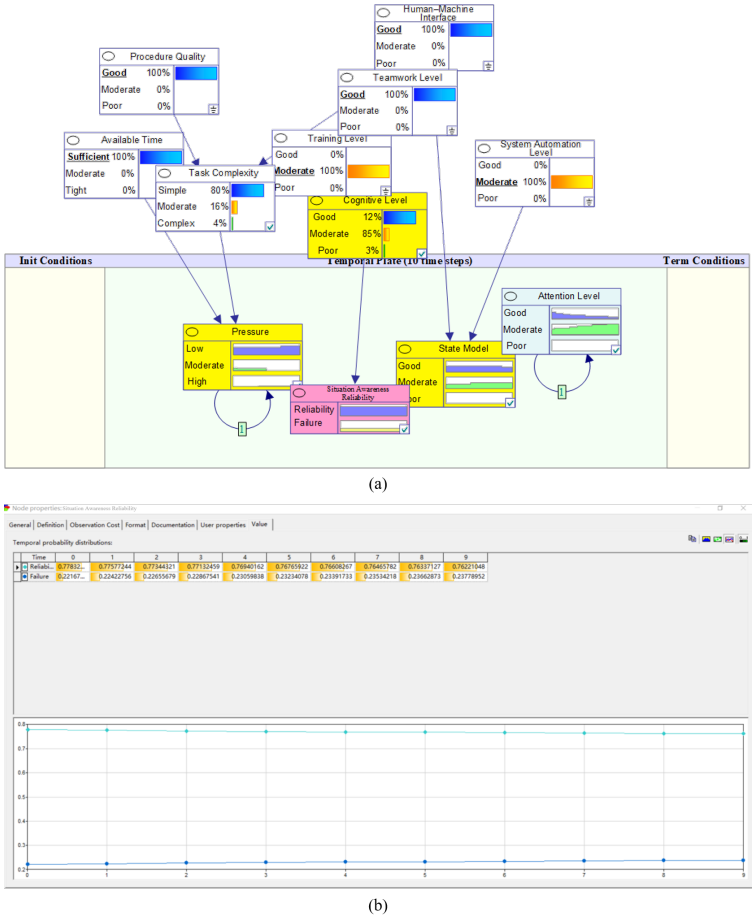

Figure 4: (a) Computational architecture of the proposed model, illustrating the flow of input features, intermediate processing layers, and probabilistic outputs. (b) Quantitative results of situation awareness (SA) reliability, showing the estimated probabilities and their temporal variations across task phases.

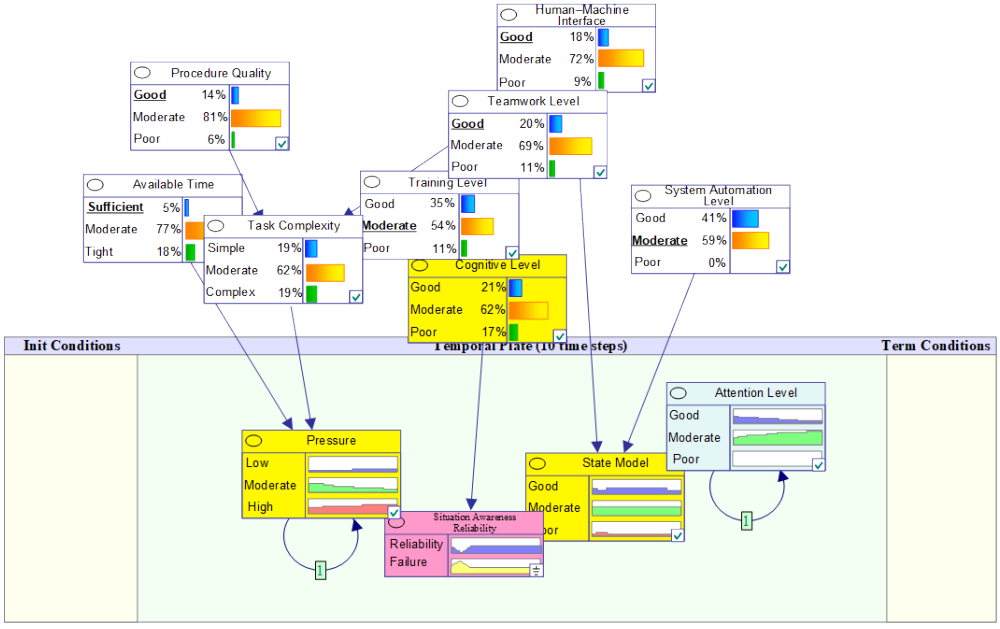

Figure 5: Temporal evolution of operator SA reliability inferred by the DBN model.

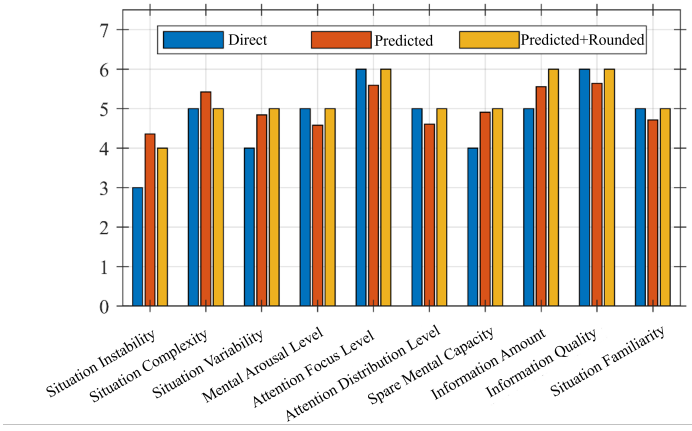

Figure 6: SART score metrics computed by the momentary prediction model.

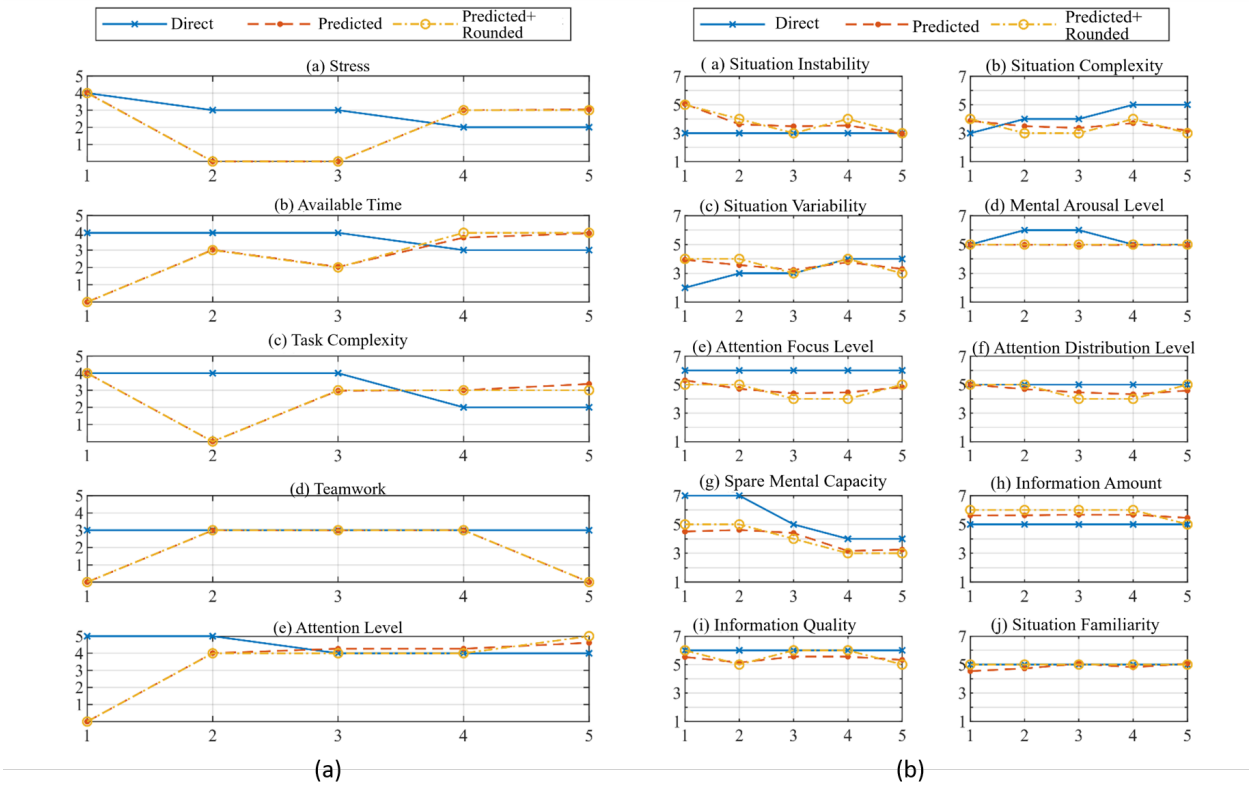

Figure 7: Outputs of the period-based prediction model: (a) dynamic influencing factors; (b) situation awareness evaluation results.

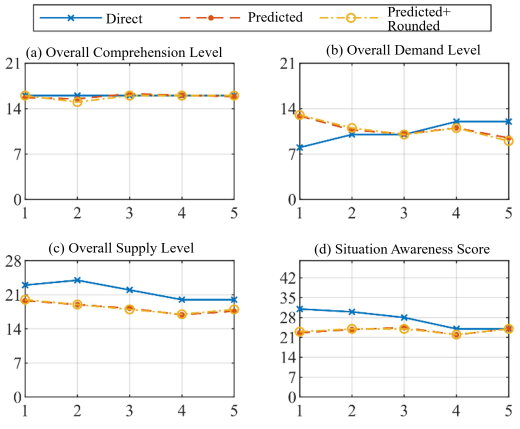

Figure 8: Final Situation Awareness Result.

SAGAT Questionnaire

Scenario: Small-Break Steam Generator Tube Rupture (SGTR) — SG1 damaged, SG2 and SG3 normal

Pause Point 1

Event: Secondary-side alarm triggered

Operator Situation Awareness Measurement Questionnaire (SGTR – First Round)

1. Will the reactor enter a shutdown condition?

☐ Yes ☐ No ☐ Uncertain

2. What type of accident do you think may have occurred?

☐ LOCA ☐ SGTR ☐ Main Steam Line Break

☐ Station Blackout ☐ Uncertain

3. Trend of primary circuit pressure:

☐ Increase ☐ Decrease ☐ Stable ☐ Uncertain

4. Trend of primary circuit water level:

☐ Increase ☐ Decrease ☐ Stable ☐ Uncertain

5. Trend of primary circuit temperature:

☐ Increase ☐ Decrease ☐ Stable ☐ Uncertain

6. Trend of containment pressure:

☐ Increase ☐ Decrease ☐ Stable ☐ Uncertain

7. Trend of containment temperature:

☐ Increase ☐ Decrease ☐ Stable ☐ Uncertain

8. Trend of containment radiation level:

☐ Increase ☐ Decrease ☐ No change ☐ Uncertain

9. Is there radioactivity detected in the secondary circuit?

☐ Yes ☐ No ☐ Uncertain

10. Pressure trend of the failed steam generator (SG):

☐ Increase ☐ Decrease ☐ Stable ☐ Uncertain

11. Pressure trend of the intact steam generators (SGs):

☐ Increase ☐ Decrease ☐ Stable ☐ Uncertain

12. Trend of steam generator water inventory:

☐ Increase ☐ Decrease ☐ Stable ☐ Uncertain

13. Status of main steam isolation valves:

☐ Isolated ☐ Not isolated ☐ Uncertain

14. Status of main coolant pumps:

☐ Three operating ☐ Two operating ☐ One operating ☐ All stopped ☐ Uncertain

15. Status of auxiliary feedwater pumps:

☐ Two motor-driven pumps ☐ Two turbine-driven pumps ☐ One motor-driven pump ☐ One turbine-driven pump ☐ Two turbine-driven + one motor-driven ☐ One turbine-driven + two motor-driven ☐ None ☐ Uncertain

16. Subcooling degree (ΔTSAT) of the primary coolant:

☐ Superheated ☐ Saturated ☐ Subcooled ☐ Uncertain

17. Reactor pressure vessel water level:

☐ Increasing ☐ Decreasing ☐ Uncertain

18. Subcriticality condition:

☐ Not degraded ☐ Degraded ☐ Uncertain

Pause Point 2

Event: Cooldown and depressurization stage (accident mitigation phase)

Operator Situation Awareness Measurement Questionnaire (SGTR – Second Round)

1. Trend of primary circuit pressure:

☐ Increase ☐ Decrease ☐ Stable ☐ Uncertain

2. Current range of primary circuit pressure:

☐ 0–50 bar ☐ 50.1–100 bar ☐ 100.1–150 bar ☐ 150.1–200 bar

3. Trend of pressurizer water level:

☐ Increase ☐ Decrease ☐ Stable ☐ Uncertain

4. Current range of pressurizer water level:

☐ Below –5 m ☐ –5 m to –3 m ☐ –3 m to 0 m ☐ 0 m to 3 m ☐ Above 3 m

5. Trend of primary circuit temperature:

☐ Increase ☐ Decrease ☐ Stable ☐ Uncertain

6. Current range of primary coolant temperature (Tric):

☐ Below 280° C ☐ 280–290° C ☐ 290–300° C ☐ Above 300° C

7. Trend of containment pressure: ☐ Increase ☐ Decrease ☐ Stable ☐ Uncertain

8. Current range of containment pressure:

☐ <1.1 bar(a) ☐ 1.1–1.3 bar(a) ☐ 1.3–2.4 bar(a) ☐ >2.4 bar(a)

9. Subcooling degree (ΔTSAT) of the primary coolant:

☐ Superheated ☐ Saturated ☐ Subcooled ☐ Uncertain

10. Current range of ΔTSAT:

☐ Below –100° C ☐ –100° C to 0° C ☐ 0° C to 50° C ☐ 50° C to 150° C ☐ Above 150° C

11. Status of main coolant pumps:

☐ Three operating ☐ Two operating ☐ One operating ☐ All stopped ☐ Uncertain

12. Number of containment spray pumps operating:

☐ Three ☐ Two ☐ One ☐ None ☐ Uncertain

13. Status of safety injection system:

☐ Two high-pressure pumps operating ☐ One high-pressure pump operating ☐ BIT isolated ☐ Uncertain

14. Pressure trend of the failed SG:

☐ Increase ☐ Decrease ☐ Stable ☐ Uncertain

15. Current range of failed SG pressure: ☐ Below 30 bar ☐ 30–50 bar ☐ 50–60 bar ☐ 60–76 bar ☐ Above 76 bar

16. Pressure trend of normal SGs:

☐ Increase ☐ Decrease ☐ Stable ☐ Uncertain

17. Status of main steam isolation valve (VVP):

☐ Isolated ☐ Not isolated ☐ Uncertain

18. Current range of normal SG pressure (for two intact SGs, fill both):

☐ Below 30 bar ☐ 30–50 bar ☐ 50–60 bar ☐ 60–76 bar ☐ Above 76 bar (x2)

19. Pressure trend of normal SGs:

☐ Increase ☐ Decrease ☐ Stable ☐ Uncertain

20. Water inventory trend of the failed SG:

☐ Increase ☐ Decrease ☐ Stable ☐ Uncertain

21. Narrow-range water level of failed SG:

☐ Below –1.8 m ☐ –1.8 m to –0.9 m ☐ –0.9 m to 0 m ☐ 0 m to 0.9 m ☐ Above 0.9 m

22. Water inventory trend of normal SGs (x2):

☐ Increase ☐ Decrease ☐ Stable ☐ Uncertain

23. Narrow-range water level of normal SGs (x2):

☐ Below –1.8 m ☐ –1.8 m to –0.9 m ☐ –0.9 m to 0 m ☐ 0 m to 0.9 m ☐ Above 0.9 m

24. Trend of containment temperature:

☐ Increase ☐ Decrease ☐ Stable ☐ Uncertain

25. Is there a radiation alarm in the secondary circuit?

☐ Yes ☐ No ☐ Uncertain

26. Status of auxiliary feedwater pumps:

☐ Two motor-driven pumps ☐ Two turbine-driven pumps ☐ One motor-driven pump ☐ One turbine-driven pump ☐ Two turbine-driven + one motor-driven ☐ One turbine-driven + two motor-driven ☐ None ☐ Uncertain

27. Subcriticality condition:

☐ Not degraded ☐ Degraded ☐ Uncertain

28. Indication range of intermediate-range detector (013MA):

☐ 10^{-11} A ☐ 10^{-10} A ☐ 10^{-9} A ☐ 10^{-8} A ☐ 10^{-7} A ☐ Above 10^{-7}

Figure 9: Formatted SAGAT Questionnaire for SGTR Scenario.